Enhanced photoluminescence of InGaAs/GaAs quantum dots induced by nanoprobe pressure effects

Kazunari Ozasa[a] and Yoshinobu Aoyagi
RIKEN (The Institute of Physical and Chemical Research), 2-1 Hirosawa, Wako, Saitama 351-0198, Japan and CREST (JST), 3-1-6-5 Shibuya, Tokyo 150-0002, Japan

Akihiko Yamane and Yoshio Arai
Engineering Department, Saitama University, Shimo-ohkubo 255, Saitama 338-8570, Japan

(Received 7 April 2003; accepted 25 June 2003)

Marked enhancement of photoluminescence of InGaAs/GaAs quantum dots (QDs) was observed by the nanoindentation of the light-collecting fiber nanoprobe onto the sample surface. In order to analyze its mechanism, calculations of the nanoprobe-induced strain and the energy-band profiles in the bulk GaAs surrounding InGaAs QDs have been performed on the bases of linear continuum elastic theory and six-band strain Hamiltonian. The calculations have revealed that the confinement potential for light holes was generated by the nanoprobe indentation. The results obtained in this study show that nanometer-scale strain modulation by nanoprobe indentation has potential for the investigation of semiconductor nanostructure physics. © *2003 American Institute of Physics.*
[DOI: 10.1063/1.1604464]

Nanoprobe measurement techniques such as scanning tunneling microscopy (STM) and atomic force microscopy have considerably contributed to the atomic-scale surface physics/chemistry. Not only the surface physics but also the optical physics of semiconductor nanostructures has developed greatly with scanning near-field optical microscopy (SNOM).[1,2] Nanoprobes can also be used to perturb/modulate the surface potential or energy bands of semiconductors, as we have demonstrated recently in the nanoprobe photoluminescence (PL) measurements of quasi-zero-dimensional InGaAs(P)/GaAs quantum dots (QDs).[3,4] In these measurements, we have found that the photoluminescence from the QDs was enhanced markedly by a small indentation of the nanoprobe onto the sample surface. In this letter, we present the enhancement of nanoprobe PL of the QDs and discuss its mechanism through the calculation of nanoprobe-induced energy-band modulation.

The apparatus we used to measure the PL of the QDs was a STM-based low-temperature (10 K) SNOM (Unisoku, USM-100R), where the nanoprobe (Au-coated optical fiber with an aperture of 500–3000 nm diameter with similar apex radius) was installed to obtain the photoluminescence through its aperture (collection mode).[3,4] A YAG2 laser (532 nm, 540 mW/cm^2) excited photocarriers in GaAs, and the obtained photoluminescence was analyzed by a monochromator (SPEX, 270M) and a charge coupled device (CCD) detector (SPEX, CCD-2000). The $In_{0.5}Ga_{0.5}As$/GaAs QDs were prepared by the strain-induced self-assembly technique (with chemical beam epitaxy at 480 °C),[5,6] and capped by 50-nm-thick GaAs. Figure 1 shows the PL enhancement observed by the nanoprobe indentation onto the sample surface. In this report, we use the term ''nanoprobe indentation'' to describe the pressing down of a nanoprobe onto the sample surface within its elastic limit (thus, no trace remains after releasing the nanoprobe). The indentation was controlled by conventional ferroelectric lead zirconate titanate devices in our STM–PL apparatus; thus, the intensity of the indentation was indicated by the nominal distance between the nanoprobe and the surface. Two points should be noted: the negative nominal distance in Fig. 1 does not mean an indentation of the material surface (the nanoprobe did not penetrate into the sample), but means that the material itself is pushed downward with minor surface indentation (the sample surface is pressed down and displaces downwards); each spectrum was reproduced repeatedly according to the nanoprobe position (up/down), which reveals that neither the sample nor the nanoprobe was destroyed by the repeated indentation. It has been clarified that the fine PL peaks originating from the individual QDs were observed to have one order of magnitude higher intensities in the case with the nanoprobe indentation (-50 nm) than the far-field broad peak ($+50$ to $+350$ nm), and that the energy of each fine PL peak shifted to higher energies by the indentation (0 to -100 nm). The maximum shifts of approximately 100 meV were observed in various experiments of the nanoprobe indentation, and parabolic traces were obtained in the scan diagram (Fig. 2), when the nanoprobe was scanned laterally with the indentation of -50 nm. The number of fine peaks observed in Fig. 1 was 30–50, which corresponds to the number of QDs within the diameter approximately 300 nm, calculated from the QD density ($5-6\times10^{10}$ cm^{-2}). The diameter 300 nm was also derived from the maximum length of peak traces in Fig. 2, and gives the effective aperture diameter of the nanoprobe.

In many research works on near-field optical physics, the enhancements of the electric field of irradiated lights due to the surface plasmon generated on the metallic surfaces of nanoparticles or nanoprobes have been reported.[7,8] The effects of the surface plasmon depend strongly on the polarization of illuminated lights.[8,9] We have also observed that the PL intensity for the *p*-polarized laser excitation is 1.8 times higher than that for *s*-polarized laser excitation (not shown

[a]Electronic mail: ozasa@postman.riken.go.jp

 © 2003 American Institute of Physics
Downloaded 10 Sep 2008 to 133.38.242.20. Redistribution subject to AIP license or copyright; see http://apl.aip.org/apl/copyright.jsp

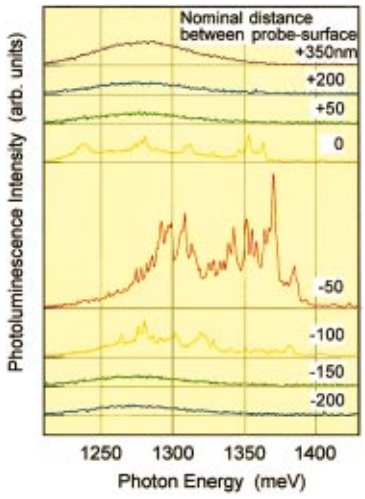

FIG. 1. (Color) Enhancement of nanoprobe photoluminescence of InGaAs QDs (not normalized).

here).[10] However, a similar polarization dependence was obtained even when the nanoprobe was positioned far away from the sample surface (+50 to +350 nm), indicating that the PL enhancement in Fig. 1 is not caused by the surface plasmon effects. The increases in PL intensity as well as the peak-energy shifts and Γ–X transitions by pressure were reported for the QDs.[11–14] Those reports describe mainly three-dimensional (3D) uniform hydrostatic pressure effects.[11–13] Since the nanoprobe-induced pressures/strains are nonuniformly distributed, the 3D analysis of the strain distribution is required to clarify the nanoprobe-indentation effects.

In order to calculate the nanoprobe-induced strains, on the basis of linear continuum elastic theory, we have assumed the apex of the nanoprobe is spherical with a 500 nm radius, and the applied Hertzian contact theory[15] (without friction), which gives a contacting radius and pressure distribution on the sample surface for a given indentation force. Considering that strain induced by InGaAs QDs is minor in the surrounding GaAs compared with that by the nanoprobe indentation, we neglected the QD layer in our strain calculations. The distribution of strain in the sample can be obtained then by using the stress-integral functions for semi-infinite

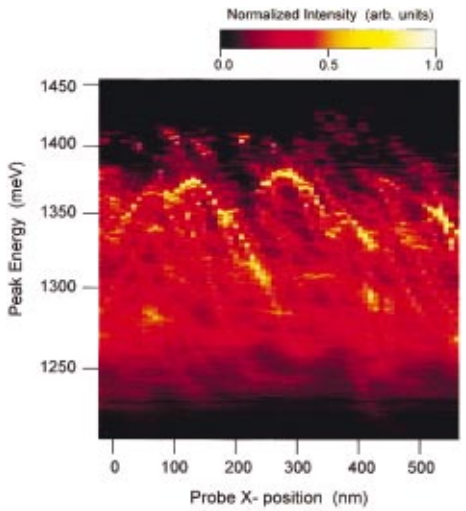

FIG. 2. (Color) Photoluminescence diagram with nanoprobe horizontal line scan.

TABLE I. Material parameters used in the calculations of strain distribution and strain Hamiltonian.

	GaAs	$In_{0.5}Ga_{0.5}As$
c_{11} (N/m^2)	11.88×10^{10}	
c_{12} (N/m^2)	5.38×10^{10}	
a_c (eV)	−7.63	−6.06
a_v (eV)	−1.00	−0.93
b (eV)	−1.77	−1.81
d (eV)	−3.10	−3.21
Δ_o (eV)	0.33	0.35

bulk.[16,17] The strain Hamiltonian of Pikus and Bir[18] was used to calculate the 3D energy-band shifts of GaAs, beneath/around the indented nanoprobe. In principle, the strain Hamiltonian of Pikus cannot be applied to nonuniformly distributed strains.[19] However, the spatial change of the nanoprobe-induced strain calculated here was moderate (less than 0.2% for 10 nm, around 50 nm depth), allowing us reasonably to apply the Pikus strain Hamiltonian. We chose the six-band strain Hamiltonian[20,21] because our main interest was to analyze the band gaps of GaAs bulk, not those of InGaAs QDs, where the eight-band Hamiltonian may be suitable. The material parameters used are listed in Table I. Elastic constants were obtained from Refs. 22 and 23, and deformation potentials from Ref. 24. Poisson ratio of 0.17[25] was used for fiber probe (quartz). Parameters for InGaAs were obtained by linear interpolation between those of GaAs and InAs.[24] The indentation force was chosen so as to reproduce a 100 meV blueshift in the InGaAs energy gap (bulk) at 50 nm beneath the nanoprobe, which corresponds to the experimental results, i.e., approximately 100 meV maximum PL peak shifts for InGaAs QDs embedded in 50-nm-thick GaAs. The maximum pressure beneath the probe, total indentation force, and contact radius calculated were 62 GPa, 173 μN, and 116 nm, respectively. The calculation process will be described in detail in a separate report.[10]

Figure 3 shows the calculated depth profiles of shifts of energy-band edges (Γ point, ΔE_c, ΔE_{hh}, ΔE_{lh}) of GaAs surrounding InGaAs QDs, together with the strain distributions (insets). The remarkable feature in Fig. 3 is that a potential minimum over 100 meV is generated for light holes at around 65 nm beneath the nanoprobe. The potential mini-

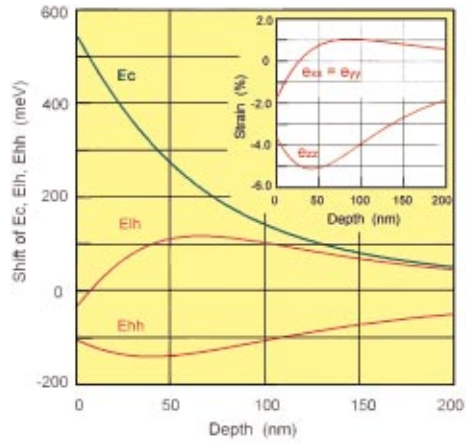

FIG. 3. (Color) Energy shift of GaAs Γ-point (E_c, E_{lh}, E_{hh}) induced by nanoprobe indentation for depth direction. Strain components are given in the insets.

Downloaded 10 Sep 2008 to 133.38.242.20. Redistribution subject to AIP license or copyright; see http://apl.aip.org/apl/copyright.jsp

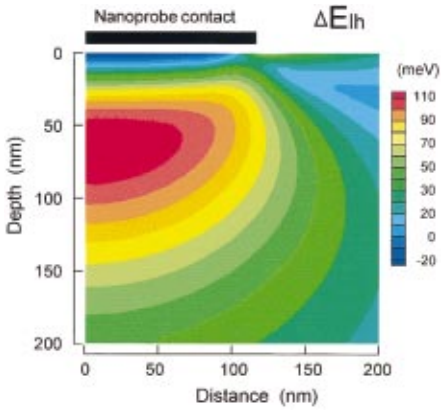

FIG. 4. (Color) Calculated depth-distance profile of energy shift of E_{lh}. Origin of distance is the center of nanoprobe apex. Nanoprobe contact area is shown by a black rectangle.

mum for light holes originates from the shear component of the strain, as shown in the inset in Fig. 3. Furthermore, the depth-distance profile of ΔE_{lh} (Fig. 4) indicates that the photoexcited light holes in the surrounding hemisphere area (approximately 300 nm horizontal diameter) flow into the potential minimum beneath the nanoprobe. Therefore, the nanoprobe-induced potential minimum for light holes in GaAs yields a higher concentration of holes than that in the case without the nanoprobe indentation. The confinement potential in our QDs of $In_{0.5}Ga_{0.5}As/GaAs$ was estimated from Ref. 26 to be 124 meV for holes and 166 meV for electrons, taking into account the measured PL peak energy without nanoprobe indentation (1.287 eV) as well as 100 meV blueshift, and assuming a linear dependence of confinement potential on composition. Since the photoexcited electrons are captured in the deeper confinement potentials than holes, the repulsive potential slopes ΔE_c in GaAs that are generated by the nanoprobe indentation (Figs. 3 and 4) negligibly affect the electron concentration in the QDs. The shape of the light hole confinement (Fig. 4) is a deformed oval or hemisphere with approximately 200 nm diameter and 70 nm depth. The smaller diameter of the confinement than the aperture of the nanoprobe (more than 500 nm) contributes to a better spatial resolution of 300 nm (effective aperture) than that expected from the probe aperture (500 nm) in our nanoprobe PL measurements.

The indentation force dependence of the shifts of E_{lh} (calculated) are shown in Fig. 5. The potential minimum for light holes changes its position (depth) according to the indentation force. The dependence explains the disappearance of the PL enhancement beyond a certain indentation of the nanoprobe (over -150 nm in nominal distance in Fig. 1), since the position of hole confinement (potential minimum) becomes off-tuned from the QD depth (50 nm). The dependence also supports our conclusion that the hole concentration is the major factor responsible for the PL enhancement, since the indentation force does not change the direction/trend of the ΔE_c slope in Fig. 3, contrary to the disappearance of the PL enhancement.

We consider that the shape and depth/position of the

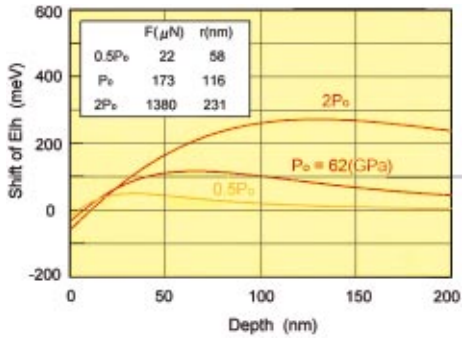

FIG. 5. (Color) Dependence of energy shift (E_{lh}) on the indentation force for depth direction. P_0, F, and r represent pressure maximum beneath the probe, total indentation force, and contact radius, respectively.

confinement potential can be tailored by the shape of nanoprobe apex and the indentation force. The results obtained in this study show high potential of nanoprobe modulation of semiconductor energy bands, where nanometer-scale modulation can be realized with microNewton indentation force, unlike in the case of conventional uniaxial pressure experiments. The nanoprobe-pressure-modulation measurements[27] of semiconductor characteristics must be useful to investigate the nanometer-scale physics in various nanostructures, especially those embedded by a thin capping layer.

[1] Y. Toda, T. Sugimoto, M. Nishioka, and Y. Arakawa, Appl. Phys. Lett. **76**, 3887 (2000).
[2] N. Hoska and T. Saiki, J. Microsc. **202**, 362 (2001).
[3] K. Ozasa, S. Nomura, and Y. Aoyagi, Superlattices Microstruct. **30**, 169 (2001).
[4] K. Ozasa and Y. Aoyagi, Physica E (Amsterdam) **13**, 212 (2002).
[5] K. Ozasa, Y. Aoyagi, Y. J. Park, and L. Samuelson, Appl. Phys. Lett. **71**, 797 (1997).
[6] K. Ozasa and Y. Aoyagi, J. Cryst. Growth **188**, 370 (1998).
[7] N. E. Hecker, R. A. Hopfel, N. Sawaki, T. Maier, and G. Strasser, Appl. Phys. Lett. **75**, 1577 (1999).
[8] N. Hayazawa, A. Tarun, Y. Inouye, and S. Kawata, J. Appl. Phys. **92**, 6983 (2002).
[9] T. Okamoto and I. Yamaguchi, Opt. Rev. **6**, 211 (1999).
[10] K. Ozasa, Y. Aoyagi, M. Maeda, M. Hara, A. Yamane, and Y. Arai (unpublished).
[11] J. L. Sly and D. J. Dunstan, Phys. Rev. B **53**, 10116 (1996).
[12] I. E. Itskevich, S. G. Lyapin, I. A. Troyan, P. C. Klipstein, L. Eaves, P. C. Main, and M. Henini, Phys. Rev. B **58**, R4250 (1998).
[13] J. Phillips, P. Bhattacharya, and U. Venkateswaran, Appl. Phys. Lett. **74**, 1549 (1999).
[14] A. C.- Pirson, J. Temmyo, and H. Ando, Physica E (Amsterdam) **7**, 367 (2000).
[15] H. Hertz, J. Reine Angew. Math. **92**, 156 (1882).
[16] J. Boussinesq, *Application des Potentials a Letude de Lequilibre et du Mouvement des Solides Elastiques* (Gauthier-Villars, Paris, 1885).
[17] I. Nakahara, T. Shibuya, E. Tsuchida, H. Kasano, T. Tsuji, and H. Inoue, *Elasticity Handbook* (Asakura, Tokyo, 2001), p. 315 (in Japanese).
[18] G. E. Pikus and G. L. Bir, Sov. Phys. Solid State **1**, 1502 (1959).
[19] T. Suzuki, Phys. Rev. B **64**, 233310 (2001).
[20] F. H. Pollak and M. Cardona, Phys. Rev. **172**, 816 (1968).
[21] C. Pryor, Phys. Rev. B **57**, 7190 (1998).
[22] S. Adachi, J. Appl. Phys. **53**, 8775 (1982).
[23] H. Jiang and J. Singh, Phys. Rev. B **56**, 4696 (1997).
[24] L. W. Wang, A. J. Williamson, A. Zunger, H. Jiang, and J. Singh, Appl. Phys. Lett. **76**, 339 (2000).
[25] E. H. Bogardus, J. Appl. Phys. **36**, 2504 (1965).
[26] L. W. Wang, J. Kim, and A. Zunger, Phys. Rev. B **59**, 5678 (1999).
[27] K. Ozasa, T. Meguro, Y. Aoyagi, A. Hida, and K. Maeda, Jpn. Patent, Appl. No. 2001-279406 (2001).

Downloaded 10 Sep 2008 to 133.38.242.20. Redistribution subject to AIP license or copyright; see http://apl.aip.org/apl/copyright.jsp